

CRAMÉR-RAO BOUNDS FOR COMPOUND-GAUSSIAN CLUTTER AND TARGET PARAMETERS

Jian Wang[†] Aleksandar Dogandžić[‡] Arye Nehorai[†]

[†] ECE Department, University of Illinois at Chicago, 851 S. Morgan St., Chicago, IL 60607

[‡] ECpE Department, Iowa State University, 3119 Coover Hall, Ames, IA 50011

Email: {jwang, nehorai}@ece.uic.edu ald@iastate.edu

ABSTRACT

We compute Cramér-Rao bounds (CRBs) for the target and compound-Gaussian clutter parameters using radar array measurements. In particular, we compute CRBs for (i) complex target amplitudes, (ii) spatial covariance matrix of the speckle component, and (iii) texture distribution parameters. We first derive general CRB expressions under an arbitrary texture model and simplify them for gamma and inverse gamma texture distributions. We use the generalized Gauss-Laguerre quadrature to compute the CRBs for gamma texture whereas the CRBs for inverse-gamma texture do not require numerical integration. We use numerical simulations to validate our results.

1. INTRODUCTION

High-resolution and low grazing angle radars give rise to small scattering cell sizes. As a result, the scattering can no longer be approximated as a Gaussian process due to the fact that the number of scatterers in a given cell is random [4]. Compound-Gaussian models have been used to characterize heavy-tailed clutter distributions in radar [1]–[5] and other applications such as speech waveform modeling, fast fading channels and various radio propagation channel disturbances as well, see [1] and references therein. The Cramér-Rao bound (CRB) is a standard benchmark for assessing estimation performance and designing systems. Modified CRB (MCRB) expressions have been derived in [5] for clutter parameters in a mixture of compound-Gaussian and Gaussian clutters and thermal noise. In this paper, we derive *exact CRBs* for target and compound-Gaussian clutter parameters.

In Section 2, we introduce the measurement scenarios with gamma [2]–[4] and inverse-gamma [2] texture models. We present the general CRB results for compound-Gaussian models in Section 3 and apply them to the two texture models in Section 4. In Section 5, we evaluate our results via numerical methods.

The work of A. Nehorai and J. Wang was supported by the Air Force Office of Scientific Research Grants F49620-02-1-0339 and FA9550-05-1-0018.

2. MEASUREMENT MODEL

We adopt the radar array measurement model for compound-Gaussian clutter in [2]. Assume that an n -element radar array receives P pulse returns, where each pulse provides N range-gate samples. We collect the spatio-temporal data from the t th range gate into a vector $\mathbf{y}(t)$ of size $m = nP$ and model $\mathbf{y}(t)$ as (see e.g. [2] and [6])

$$\mathbf{y}(t) = A\mathbf{X}\phi(t) + \mathbf{e}(t), \quad t = 1, \dots, N \quad (1)$$

where A is an $m \times r$ spatio-temporal steering matrix of the targets, $\Phi = [\phi(1), \phi(2), \dots, \phi(N)]$ is the temporal response matrix, X is an $r \times d$ matrix of unknown complex amplitudes of the targets, and $\mathbf{e}(t)$ is additive independent identically distributed (i.i.d.) *compound-Gaussian clutter*, see e.g. [2]–[4]. We now represent the above measurement scenario using the following model: $\mathbf{y}(t)$, $t = 1, 2, \dots, N$ are conditionally independent random vectors with complex Gaussian probability density functions (pdfs):

$$p_{\mathbf{y}|u}(\mathbf{y}(t) | u(t); X, \Sigma) = \exp \left\{ -[\mathbf{y}(t) - A\mathbf{X}\phi(t)]^H \cdot [u(t)\Sigma]^{-1} \cdot [\mathbf{y}(t) - A\mathbf{X}\phi(t)] \right\} / |\pi u(t)\Sigma| \quad (2)$$

where “ H ” denotes the Hermitian (conjugate) transpose, Σ is the (unknown) covariance matrix of the *speckle component*, and $u(t)$, $t = 1, 2, \dots, N$ are the unobserved *texture components* (powers), modeled as i.i.d. non-negative random variables. We consider the following texture distributions:

- **gamma:** $u(t)$ follow a gamma distribution, and
- **inverse gamma:** $1/u(t)$ follow a gamma distribution.

Define the vector of signal and clutter parameters:

$$\boldsymbol{\rho} = [\boldsymbol{\xi}^T, \boldsymbol{\eta}^T, \nu]^T \quad (3a)$$

where “ T ” denotes a transpose,

$$\boldsymbol{\xi} = [\text{Re}\{\text{vec}(X)\}^T, \text{Im}\{\text{vec}(X)\}^T]^T \quad (3b)$$

$$\boldsymbol{\eta} = [\text{Re}\{\text{vech}(\Sigma)\}^T, \text{Im}\{\text{vech}(\Sigma)\}^T]^T \quad (3c)$$

and ν is the texture parameter¹. (Here, the `vech` and `vech` operators create a single column vector by stacking elements below the main diagonal columnwise; `vech` includes the main diagonal, whereas `vech` omits it.)

Our goal is to compute the CRB matrix for the unknown parameters ρ .

3. GENERAL CRB RESULTS

3.1. Preliminaries

Denote by $p_u(u(t); \nu)$ the pdf of the texture $u(t)$. Then, according to the above measurement model, $\mathbf{y}(t)$ is a complex spherically invariant random vector (SIRV) with marginal pdf

$$p_{\mathbf{y}}(\mathbf{y}(t); \rho) = \frac{1}{|\pi \Sigma|} \cdot g(\|\mathbf{z}(t; \xi, \eta)\|^2, \nu) \quad (4)$$

where

$$g(s, \nu) = \int_0^\infty \exp\left(-\frac{s}{u}\right) \cdot u^{-m} \cdot p_u(u; \nu) du \quad (5a)$$

$$\mathbf{z}(t; \xi, \eta) = \Sigma^{-1/2} \cdot [\mathbf{y}(t) - A X \phi(t)] \quad (5b)$$

and $\|\cdot\|$ denotes the Frobenius norm. Also, $\Sigma^{-1/2} = (\Sigma^{1/2})^{-1}$ where $\Sigma^{1/2}$ denotes a Hermitian square root of a Hermitian matrix Σ . Given an arbitrary radius $\|\mathbf{z}(t; \xi, \eta)\| = r$, the concatenated vector of real and imaginary parts of $\mathbf{z}(t; \xi, \eta)$ is uniformly distributed on the $2m$ -dimensional ball with radius r , centered at the origin. Denote by g_1 and g_2 the partial derivatives of $g(\cdot, \cdot)$ with respect to its first and second entries, i.e. $g_1(s, \nu) = \partial g(s, \nu) / \partial s$ and $g_2(s, \nu) = \partial g(s, \nu) / \partial \nu$. For any well-behaved $g(\cdot, \cdot)$, we can change the order of differentiation and integration, leading to

$$g_1(s, \nu) = - \int_0^\infty \exp\left(-\frac{s}{u}\right) \cdot u^{-m-1} \cdot p_u(u; \nu) du \quad (6a)$$

$$g_2(s, \nu) = \int_0^\infty \exp\left(-\frac{s}{u}\right) \cdot u^{-m} \cdot \frac{\partial p_u(u; \nu)}{\partial \nu} du. \quad (6b)$$

To derive the CRB results in this paper we utilize the following lemma, obtained by adapting the properties of real SIRVs in e.g. [7, Lemma 1] to the complex case.

Lemma: For a $\mathbf{z} = \mathbf{z}(t; \xi, \eta)$ [defined in (5b)] and any $n \times n$ matrices A and B ,

$$\mathbb{E} \left(\frac{\mathbf{z}^H}{\|\mathbf{z}\|} A \frac{\mathbf{z}}{\|\mathbf{z}\|} \middle| \|\mathbf{z}\| \right) = \frac{1}{n} \text{tr}(A) \quad (7a)$$

$$\mathbb{E} \left(\frac{\mathbf{z}^H}{\|\mathbf{z}\|} A \frac{\mathbf{z}}{\|\mathbf{z}\|} \frac{\mathbf{z}^H}{\|\mathbf{z}\|} B \frac{\mathbf{z}}{\|\mathbf{z}\|} \middle| \|\mathbf{z}\| \right) = \frac{1}{n(n+1)} [\text{tr}(AB) + \text{tr}(A) \text{tr}(B)]. \quad (7b)$$

¹We parametrize the texture pdf using only one parameter. The extension to multiple parameters is straightforward.

3.2. Results

The Fisher information matrix (FIM) for ρ is computed by using [8, eqs. (3.21) and (3.23)]:

$$[\mathcal{I}]_{\rho_i \rho_k} = \mathbb{E} \left\{ \frac{\partial \ln p(\mathbf{y}; \rho)}{\partial \rho_i} \frac{\partial \ln p(\mathbf{y}; \rho)}{\partial \rho_k} \right\} \quad (8a)$$

$$= -\mathbb{E} \left\{ \frac{\partial^2 \ln p(\mathbf{y}; \rho)}{\partial \rho_i \partial \rho_k} \right\} \quad (8b)$$

where $[\mathcal{I}]_{\rho_i \rho_k}$ denotes the FIM entry with respect to the parameters ρ_i and ρ_k , $i, k \in \{1, 2, \dots, \dim(\rho)\}$ and

$$\ln p(\mathbf{y}; \rho) = -N \ln |\pi \Sigma| + \sum_{t=1}^N \ln g(\|\mathbf{z}(t; \xi, \eta)\|^2, \nu) \quad (8c)$$

is the log-likelihood function. Then the CRB for ρ is

$$\text{CRB} = \mathcal{I}^{-1}. \quad (8d)$$

To simplify the notation, we omit the dependencies of the FIM and CRB on the model parameters. We also omit details of the derivation and give the final FIM expressions:

$$\mathcal{I}_{\xi_i \xi_k} = \frac{2\alpha_1}{m} \sum_{t=1}^N \text{Re} \left[\phi^H(t) \frac{\partial X^H}{\partial \xi_k} A^H \Sigma^{-1} A \frac{\partial X}{\partial \xi_i} \phi(t) \right] \quad (9a)$$

$$\mathcal{I}_{\eta_i \eta_k} = N^2 c_{\eta_i \eta_k} + \frac{2N^2 c_{\eta_i \eta_k}}{m} \cdot \alpha_2 + \frac{N(N-1) c_{\eta_i \eta_k}}{m^2} \cdot \alpha_2^2 + \frac{N}{m(m+1)} \left[\text{tr}(\Sigma^{-1} \frac{\partial \Sigma}{\partial \eta_i} \Sigma^{-1} \frac{\partial \Sigma}{\partial \eta_k}) + c_{\eta_i \eta_k} \right] \cdot \alpha_3 \quad (9b)$$

$$\mathcal{I}_{\nu \nu} = N \cdot \beta_1 \quad (9c)$$

$$\mathcal{I}_{\eta_i \nu} = \frac{N}{m} \text{tr} \left(\Sigma^{-1} \frac{\partial \Sigma}{\partial \eta_i} \right) \cdot \beta_2 \quad (9d)$$

$$\mathcal{I}_{\xi_i \eta_k} = 0 \quad (9e)$$

$$\mathcal{I}_{\xi_i \nu} = 0 \quad (9f)$$

$$\text{where } c_{\eta_i \eta_k} = \text{tr} \left(\Sigma^{-1} \frac{\partial \Sigma}{\partial \eta_i} \right) \text{tr} \left(\Sigma^{-1} \frac{\partial \Sigma}{\partial \eta_k} \right) \quad (10)$$

and

$$\alpha_1 = \frac{\int_0^\infty \frac{g_1^2(r^2, \nu)}{g(r^2, \nu)} \cdot r^{2m+1} dr}{\int_0^\infty g(r^2, \nu) \cdot r^{2m-1} dr} \quad (11a)$$

$$\alpha_2 = \frac{\int_0^\infty g_1^2(r^2, \nu) \cdot r^{2m+1} dr}{\int_0^\infty g(r^2, \nu) \cdot r^{2m-1} dr} \quad (11b)$$

$$\alpha_3 = \frac{\int_0^\infty \frac{g_1^2(r^2, \nu)}{g(r^2, \nu)} \cdot r^{2m+3} dr}{\int_0^\infty g(r^2, \nu) \cdot r^{2m-1} dr} \quad (11c)$$

$$\beta_1 = \frac{\int_0^\infty \left(\frac{g_2^2(r^2, \nu)}{g(r^2, \nu)} - \frac{\partial g_2(r^2, \nu)}{\partial \nu} \right) \cdot r^{2m-1} dr}{\int_0^\infty g(r^2, \nu) \cdot r^{2m-1} dr} \quad (11d)$$

$$\beta_2 = \frac{\int_0^\infty \left(\frac{\partial g_1(r^2, \nu)}{\partial \nu} - \frac{g_1(r^2, \nu) g_2(r^2, \nu)}{g(r^2, \nu)} \right) \cdot r^{2m+1} dr}{\int_0^\infty g(r^2, \nu) \cdot r^{2m-1} dr}. \quad (11e)$$

Here, (9a) and (9b) have been computed by using (8a) and the lemma, whereas (9c)-(9f) follow by using (8b).

Interestingly, FIMs of compound-Gaussian models with different texture distributions share the common structure in (9a)-(9f) where the texture-specific quantities are the scalar coefficients in (11). The above FIM and CRB matrices are block-diagonal [see (9e) and (9f)], implying that the CRBs for the signal parameters ξ are uncoupled from the clutter parameters ν and η . Hence, the CRB matrix for ξ remains the same whether or not ν and Σ are known. Similarly, the CRBs for η and ν remain the same whether or not X is known. Also, (9a) and (9b) simplify to the FIM expressions for complex Gaussian clutter when $\alpha_1 = m$, $\alpha_2 = -m$ and $\alpha_3 = m(m+1)$, see also [8, eq. (15.52)].

4. CRB FOR SPECIFIC TEXTURE DISTRIBUTIONS

4.1. CRB for General Compound-Gaussian Texture

Computing the texture-specific terms in (11) typically involves two-dimensional integration that cannot be evaluated in closed form. This integration can be performed using Gauss quadratures, see e.g. [9, Ch. 5.3]. Here we use the gamma texture as an example.

Gamma texture: Assume that $u(t), t = 1, \dots, N$ follow a gamma distribution with mean one and unknown shape parameter $\nu > 0$:

$$p_u(u(t); \nu) = \frac{1}{\Gamma(\nu)} \cdot \nu^\nu u(t)^{\nu-1} \exp[-\nu u(t)]. \quad (12)$$

This choice of the texture distribution leads to the well-known K clutter model [4]. After applying a change-of-variable transformation $x = \nu u$ in (5a) and (6), we evaluate both integrals in (11) using the generalized Gauss-Laguerre quadrature formula (see [9, Ch. 5.3]):

$$\int_0^\infty f(x) \cdot x^{\nu-1} \exp(-x) dx \approx \sum_{l=1}^L w_l(\nu-1) f(x_l(\nu-1)) \quad (13)$$

where $f(x)$ is an arbitrary real function, L is the quadrature order (determining approximation accuracy), and $x_l(\nu-1)$ and $w_l(\nu-1)$, $l = 1, 2, \dots, L$ are the abscissas and weights of the generalized Gauss-Laguerre quadrature with parameter $\nu-1$. For example, the formula used to compute α_1 is given in (14), where we omit the dependencies of the abscissas and weights on $\nu-1$ to simplify the notation.

Inverse-gamma texture: Assume now that $w(t) = u(t)^{-1}$, $t = 1, 2, \dots, N$ are gamma random variables with mean one and unknown shape parameter $\nu > 0$, see also [2]. Consequently, $u(t)$ follows an inverse gamma distribution and the conditional pdf of $\mathbf{y}(t)$ given $w(t)$ is $p_{\mathbf{y}|u}(\mathbf{y}(t) | w(t))^{-1}$;

X, Σ), see (2). Integrating $w(t)$ out, we obtain a *closed-form* expression for the marginal pdf of $\mathbf{y}(t)$:

$$p_{\mathbf{y}}(\mathbf{y}(t); \rho) = \frac{\Gamma(\nu+m)}{|\pi \Sigma| \cdot \Gamma(\nu) \cdot \nu^m} \cdot \left\{ 1 + \frac{[\mathbf{y}(t) - AX\phi(t)]^H \Sigma^{-1} [\mathbf{y}(t) - AX\phi(t)]}{\nu} \right\}^{-\nu-m} \quad (15)$$

which is the *complex multivariate t distribution* with location vector $AX\phi(t)$, scale matrix Σ , and shape parameter ν , see also [2]. Interestingly, (5a) and (6) can be evaluated in closed form as well, leading to the following simple expressions for the texture-specific terms in (11a)-(11e):

$$\alpha_1 = \frac{m(\nu+m)}{\nu+m+1} \quad (16a)$$

$$\alpha_2 = -m \quad (16b)$$

$$\alpha_3 = \frac{m(m+1)(\nu+m)}{\nu+m+1} \quad (16c)$$

$$\beta_1 = \frac{\text{TG}(\nu) - \text{TG}(\nu+m)}{\nu(\nu+m)(\nu+m+1)} \quad (16d)$$

$$\beta_2 = -\frac{m}{(\nu+m)(\nu+m+1)} \quad (16e)$$

where $\text{TG}(x) = d^2[\ln \Gamma(x)]/dx^2$ is the trigamma function. Interestingly, the CRB matrix for the signal parameters ξ is proportional to the corresponding CRB matrix for complex Gaussian clutter, with the proportionality factor $(\nu+m+1)/(\nu+m)$ always greater than one.

As $\nu \rightarrow \infty$, the inverse gamma texture distribution degenerates to a constant, the marginal pdf of $\mathbf{y}(t)$ in (4) reduces to the complex Gaussian distribution in (2) with $u(t) \equiv 1$, and (9a) and (9b) simplify to the FIM expressions for complex Gaussian clutter.

5. NUMERICAL SIMULATIONS

The numerical examples presented here validate the CRB expressions for ρ using numerical simulations. We adopt the same parameter setting as in [2]: a 3-element array and $P = 3$ pulses (i.e. $m = 9$) and a rank-one target scenario with $\phi(t) \equiv 1$, $X = 0.207 \cdot \exp(j\pi/7)$, and $A = \mathbf{b}(\varpi) \otimes \mathbf{a}(\vartheta)$, where $\mathbf{b}(\varpi) = [1, \exp(j2\pi\varpi), \exp(j4\pi\varpi)]^T$ with normalized Doppler frequency $\varpi = 0.42$, and $\mathbf{a}(\vartheta) = [1, \exp(j2\pi\vartheta), \exp(j4\pi\vartheta)]^T$ with a spatial frequency $\vartheta = 0.926$. Here, \otimes denotes the Kronecker product. The speckle covariance matrix Σ was generated using a model similar to that in [10, Sec. 2.6] with 1000 patches; the diagonal elements of Σ were 10.17. We apply the ML method in [2]

$$\alpha_1 = \left[\sum_{l_1=1}^L \frac{(\sum_{l_2=1}^L \exp(-\frac{\nu x_{l_1}^2}{x_{l_2}}) \nu x_{l_2}^{-(m+1)} \cdot w_{l_2})^2}{\sum_{l_3=1}^L \exp(-\frac{\nu x_{l_1}^2}{x_{l_3}}) x_{l_3}^{-m} \cdot w_{l_3}} \exp(x_{l_1}) \cdot w_{l_1} \right] / \left[\sum_{l_4=1}^L (\sum_{l_5=1}^L \exp(-\frac{\nu x_{l_4}^2}{x_{l_5}}) x_{l_5}^{-m} \cdot w_{l_5}) \exp(x_{l_4}) \cdot w_{l_4} \right]. \quad (14)$$

to estimate the unknown parameters and compare the average mean-square errors (MSEs) of the ML estimates of ξ , η , and ν (computed using 1000 independent trials) with the corresponding CRBs derived in this paper. (Here, averaging is performed over the elements of ξ and η .)

We first consider the gamma texture model with the shape parameter $\nu = 2$. The quadrature order of the generalized Gauss-Laguerre approximation was $L = 50$. Figure 1 shows the average MSEs and CRBs for the ML estimates of the unknown parameters as functions of the number of range samples (snapshots) N . Figure 2 compares the average MSEs and corresponding CRBs for the inverse-gamma texture model with the shape parameter $\nu = 4$.

The simulation results show that the ML estimates of ξ and η are almost efficient, having MSEs close to the corresponding CRBs, and the ML estimates of ν are asymptotically efficient, as expected.

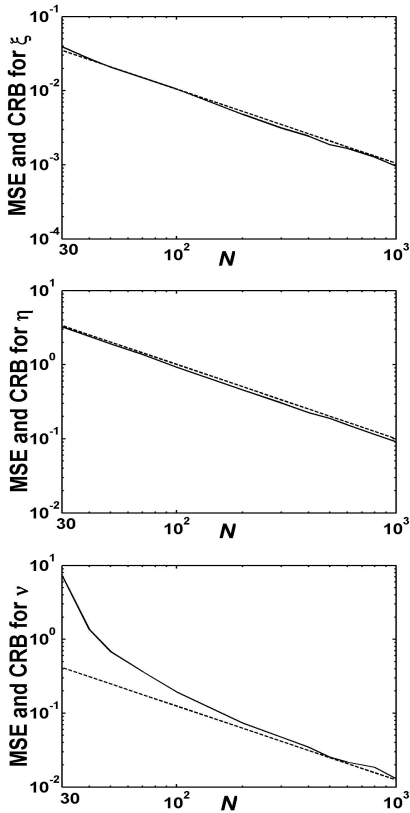


Fig. 1. Average MSEs for the ML estimates of ξ , η , and ν (solid lines) and corresponding CRBs (dashed lines) under the gamma texture model (K clutter), as functions of N .

6. REFERENCES

[1] K. Yao, "Spherically invariant random processes: Theory and applications," in *Communications, Information and Network Security*, V.K. Bhargava *et al.*, Eds., Dordrecht, The Netherlands: Kluwer Academic Publishers, 2002, pp. 315–332, ch. 16.

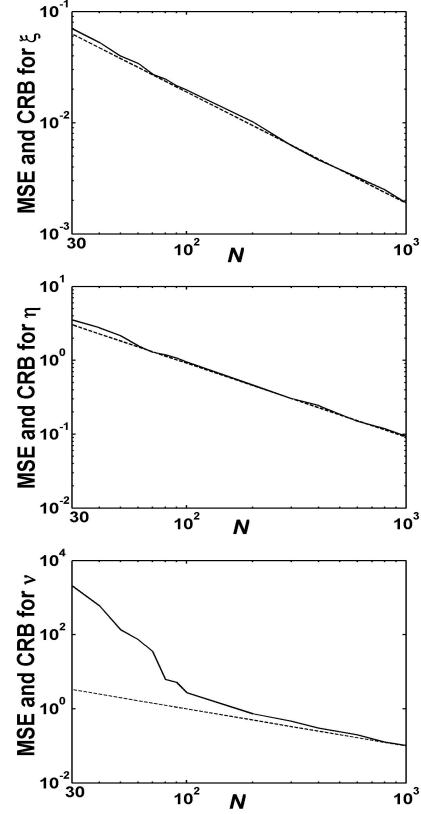


Fig. 2. Average MSEs for the ML estimates of ξ , η , and ν (solid lines) and corresponding CRBs (dashed lines) under the inverse-gamma texture model, as functions of N .

[2] A. Dogandžić, A. Nehorai, and J. Wang, "Maximum likelihood estimation of compound-Gaussian clutter and target parameters," in *Proc. 12th Annu. Workshop Adaptive Sensor Array Processing*, Lexington, MA, Mar. 2004.

[3] V. Anastassopoulos, G.A. Lampropoulos, A. Drosopoulos, and N. Rey, "High resolution radar clutter statistics," *IEEE Trans. Aerosp. Electron. Syst.*, vol. 35, pp. 43–60, Jan. 1999.

[4] K.J. Sangston and K.R. Gerlach, "Coherent detection of radar targets in a non-Gaussian background," *IEEE Trans. Aerosp. Electron. Syst.*, vol. 30, pp. 330–340, April 1994.

[5] F. Gini, "A radar application for modified Cramér-Rao bound: Parameter estimation in non-Gaussian clutter," *IEEE Trans. Signal Processing*, vol. 46, pp. 1945–1953, July 1998.

[6] A. Dogandžić and A. Nehorai, "Generalized multivariate analysis of variance: A unified framework for signal processing in correlated noise," *IEEE Signal Processing Mag.*, vol. 20, pp. 39–54, Sept. 2003.

[7] K.L. Lange, R.J.A. Little, and J.M.G. Taylor, "Robust statistical modeling using the t distribution," *J. Amer. Stat. Assoc.*, vol. 84, pp. 881–896, Dec. 1989.

[8] S.M. Kay, *Fundamentals of Statistical Signal Processing — Estimation Theory*, Prentice-Hall, 1993.

[9] R.A. Thisted, *Elements of Statistical Computing: Numerical Computation*, New York: Chapman & Hall, 1988.

[10] J. Ward, *Space-Time Adaptive Processing for Airborne Radar*, Lincoln Lab., Tech. Report 1015, MIT, Dec. 1994.